Structure and interaction mechanism in the magic $Al_{13}^{+}H_2O$ cluster

Q. Sun, Q. Wang, J. Z. Yu, T. M. Briere, and Y. Kawazoe
Institute for Materials Research, Tohoku University, Sendai 980-8577, Japan
(Received 9 July 2001; published 12 October 2001)

In order to explain the experimental observation of the magic $Al_{13}^{+}H_2O$ cluster [T. P. Lippa *et al.*, Chem. Phys. Lett. **305**, 75, (1999)], first-principles calculations are performed, a new stable structure for Al_{13}^{+} is found, and its intrinsic stability is confirmed. The most preferable adsorption site for the water molecule is determined from the electronic structure, and the interaction mechanism is clarified: the p_z lone electron pair in the H_2O molecule dominates the interactions with Al_{13}^{+} over the p_x lone electron pair. Due to the strong interaction of the lone electron pair of the water molecule with the Al_{13}^{+} cluster, the adsorption energy for this molecule is 1.77 eV, and the adsorption widens the highest occupied-lowest unoccupied molecular orbital (HOMO-LUMO) gap in $Al_{13}^{+}H_2O$ to 1.63 eV, which contributes to the stability of this cluster.

DOI: 10.1103/PhysRevA.64.053203 PACS number(s): 36.40.Mr

I. INTRODUCTION

The discovery of magic numbers in Na_n clusters [1] launched a new era in cluster science and technology, which promises exciting possibilities of designing materials with certain desired properties by using *size* as an extra degree of freedom. In particular, magic clusters with closed electron shells can be viewed as superatoms, and by assembling these superatoms, a novel class of materials with tailored properties can be synthesized [2]. Therefore, the question of how to design such superatoms demands great attention. The number of valence electrons in a cluster can be easily altered either by changing the size, composition, or charge in such a way that it may have the same electronic configuration as an atom in the periodic table, which provides an unprecedented opportunity to design a cluster as a superatom. A typical example of this occurs in Al cluster. Bulk Al is a nearly-free-electron metal, where the deviations from free-electron energy levels occur only near the Brillouin-zone boundaries. The electronic structures of Al clusters are, therefore, expected to be described by the jellium model as alkali metal clusters [3]. However, Al is a trivalent atom and it is impossible to choose a neutral Al cluster containing fewer than 46 atoms whose valence electrons equal any of the magic numbers for alkali metal clusters. Doping or charging is thus required to create the magic clusters. For example, the stabilities of Al_{13}^{-}, $Al_{12}Si$, $Al_{12}C$, $Al_{13}H$, and $Al_{13}K$ clusters have been explained by relating their electronic structure to closed electronic shells with 40 valence electrons. For the positively charged clusters Al_n^{+}, the magic number $n=7$ is considered as resulting from the filling of electronic shells with 20 valence electrons. Other clusters based on Al, including Al_7C^{-} [4], Al_7N [5], and Al_7CL_i [6], are also found to be magic.

Recently, the $Al_{13}^{+}H_2O$ cluster resulting from molecular adsorption of water during laser vaporization of Al was shown experimentally to be magic [7]. This intriguing result leaves many open questions to answer theoretically, such as: Why is it stable? What is the structure? How does the water molecule interact with Al cluster? Compared to doping, molecular adsorption is more complicated, due to the existence of lone electron pairs in H_2O, which makes this magic $Al_{13}^{+}H_2O$ cluster more interesting. Additionally, aluminum is the most abundant metal in the earth's crust, and water is very abundant in our surroundings; therefore, the mechanism for the interaction of the H_2O molecule with Al is very important to deeply understand catalysis, corrosion, passivation, and electrochemistry. Finally, clusters can be used as models for certain surfaces, and so studies on the adsorption of H_2O on clusters can also shed some light on surface adsorption.

II. THEORETICAL METHOD

The starting point in any description of cluster properties is their geometrical structure. However, there is currently no experimental technique that can provide direct information on cluster geometry. The cluster is too large for spectroscopic techniques and too small for diffraction techniques. Although Raman spectroscopy on matrix isolated clusters has been used [8], the effect of the matrix on the cluster geometry remains a nagging concern. The only method that enables determination of cluster geometries at present is based on theoretical calculations, with the correctness of the geometries being established through comparison of calculated properties with those from experiment.

Ab initio methods based on density-functional theory (DFT) are well established tools to study structural properties of materials. In particular, the plane-wave basis and pseudopotential method combined with DFT provide a simple framework, in which the calculation of forces is greatly simplified to enable extensive geometry optimization. In the present calculations, we have used a powerful *ab initio* ultrasoft pseudopotential scheme with plane-wave basis (Vienna *Ab initio* Simulation Program) [9–11], in which the finite-temperature effect local-density functional theory developed by Mermin [12] is used, and the variational quantity is the electronic free energy. Finite temperature leads to the broadening of the electron levels that is very helpful to improve the convergence of Brillouin-zone integrations. The electron-ion interaction is described by a fully nonlocal optimized ultrasoft pseudopotential [9].

The minimization of the free energy over the degrees of

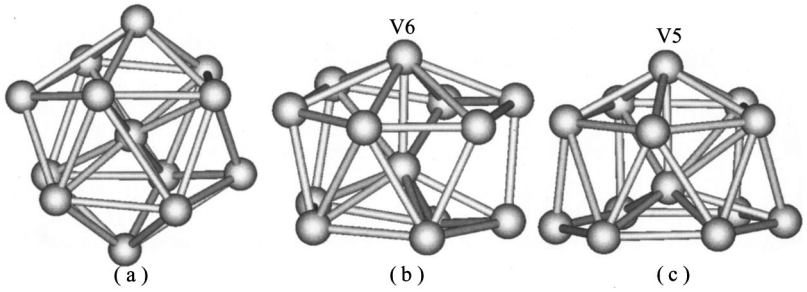

FIG. 1. Three structures of Al_{13}^{+}: config. I (a), config. II (b), and config. III (c).

freedom of the electron densities and atomic positions is performed using the conjugate-gradient iterative-minimization technique [13]. A cubic cell with edge length of structure optimization 20 Å for cluster is used and the Γ point is used to sample the Brillouin zone. The generalized gradient approximation exchange-correlation potential [14,15] is adopted. The calculations are performed with high precision, the convergence criterion for energy and force being 10^{-5} eV and 0.001 eV/Å, respectively, and the symmetry is unrestricted. Following optimization, the electronic structure of the cluster is computed using the molecular-orbital method, which allows for a detailed orbital-population analysis. Calculations are performed with GAUSSIAN 98 program [16] and employing the Becke and Lee-Yang-Parr (B3LYP) hybrid functional and 6-31+G(d,p) Gaussian basis set.

III. RESULTS AND DISCUSSIONS

In order to test the validity of our calculations, we have first performed numerical calculations on some smaller related systems and the ionization energy is found to be 5.956 eV for Al atom, which is very close to the experimental value of 5.98 eV [17]. For Al_2, the ground state is found to be $^3\Pi_u$, with bond length of 2.48 Å and a binding energy of 1.86 eV. These results are in good agreement with the experimental binding energy (1.5 eV) [18] as well as with the results obtained from other theoretical calculations [19]. For the H_2O molecule, the C—H bond length is 0.98 Å, and the H—O—H bond angle is 105.2°, in agreement with the experimental values of 0.96 Å and 104.5° [20].

A. Equilibrium geometry of Al_{13}^{+}

In order to determine the structure of the $Al_{13}^{+}H_2O$ cluster, we should first determine the structure of Al_{13}^{+}. We start with three initial structures as shown in Fig. 1; the first (config. I) has I_h symmetry, the second (config. II) is the structure found in Ref. [21], which is composed of a five-atom ring, a central atom, a six-atom ring, and a vertex atom (V6) capped on the six-atom ring, the third (config. III) differs from config. II in the exchange of the five-atom and six-atom rings, with V5 being the vertex atom. Table I shows the total binding energy, HOMO-LUMO gap, and the mean nearest-neighbor distance, from which we can see that configuration III is the most stable. The stability of this structure is confirmed further by vibrational frequency calculations, where all the frequencies are positive, suggesting this geometry is intrinsically stable. Figure 2 shows the obtained spectra. The most intensive mode corresponds to the vibration of the central atom along the direction perpendicular to the bond between the central atom and the V5 atom. The vibration with the highest frequency is mainly contributed by the V5 atom, while the vibration with the lowest frequency corresponds to the relative rotation between the five-atom ring and the six-atom ring around the bond of the central atom and the V5 atom.

TABLE I. Results for three configurations of the Al_{13}^{+} cluster. ϵ is the binding energy (in eV, defined with respect to the isolated atoms) and r is the average bond length between Al atoms in angstroms.

Structure	ϵ	HOMO-LUMO gap	r
Config. I	−30.7259	0.493	2.7603
Config. II	−30.9301	0.917	2.7606
Config. III	−31.2523	1.245	2.7088

The equilibrium geometry of the Al_{13}^{+} cluster is different from that in Ref. [21], where configuration II was found to be most stable. In fact, if we distort this structure slightly and optimize further, the final structure coincides with configuration III, which is also more symmetric than configuration II.

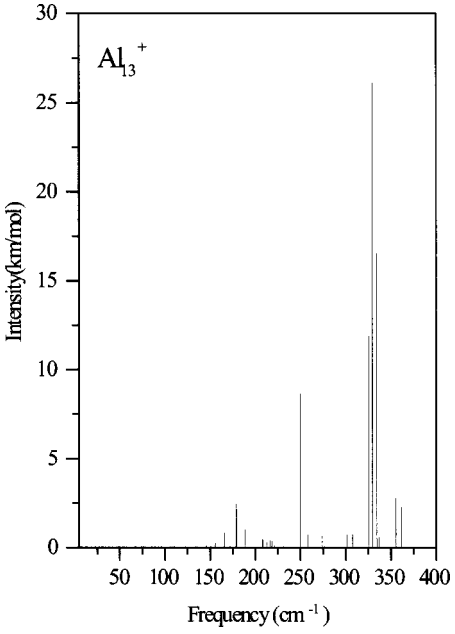

FIG. 2. Vibration spectra for Al_{13}^{+} with structure of config. III.

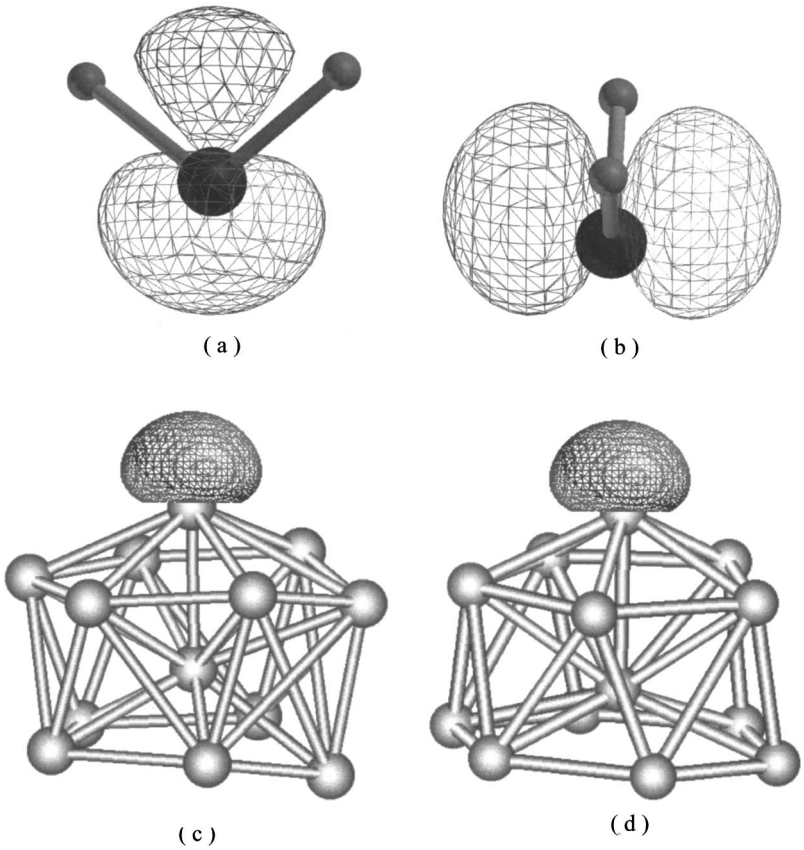

FIG. 3. The lone electron pair orbitals with predominantly p_z (a) and p_x (b) character in H_2O and the LUMO for Al_{13}^+ using config. II (c) and config. III (d). The orbitals are represented with mesh lines, and the isosurface values are 0.2, 0.2, 0.06, and 0.07, respectively.

The HOMO-LUMO gap for configuration II is 0.92 eV, in agreement with the value of 0.95 eV found in Ref. [21]; however, configuration III has a larger value of 1.245 eV, and configuration I has the smallest. The large values of the binding energy and the HOMO-LUMO gap as well as the positive vibrational frequencies establish the stability of configuration III.

B. Equilibrium geometry of $Al_{13}^+H_2O$

1. Bonding features of the water molecule

In order to determine how the H_2O molecule interacts with the Al_{13}^+ cluster, let us first recall the chemical properties of the H_2O molecule itself. The bonds that hold hydrogen and oxygen together are covalent. There are also two pairs of electrons uninvolved in the covalent bonds, and they form lone pairs, as shown in Figs. 3(a) and 3(b). If the H—O—H plane is defined as the *yz* plane, the characters of these two lone pairs can be predominantly described by the $2p_z$ and $2p_x$ orbitals of oxygen, respectively. The lone pairs contain two negative electrons each, and want to stay away from each other as much as possible. These repulsive forces push the hydrogen atoms closer together, therefore, making the water molecule bent with H—O—H bonding angle of 104.5°. The negative lone electron pairs in oxygen can interact more favorably with other substances than can the hydrogen atoms. Therefore, we consider the interactions between Al_{13}^+ and H_2O through the O atom and not through the H atoms.

2. Structure

Owing to the fact that the number of isomers increases exponentially with cluster size, it is not easy to find the global minimum for large clusters. It is also possible that adsorption can change the structure, e.g., the I_h geometry is more stable than the O_h for the Fe_{13} cluster; however, when eight oxygen atoms are adsorbed, the final structure from O_h is more stable than that from I_h [22]. Similar features are also found for the Fe_9 and Fe_9O_6 clusters [23], suggesting that in some cases the metastable structure has more freedom, relaxing to the stable structure when absorption occurs. This is due to the fact that there are some energy barriers between the different isomers. In order to search for the possible structure of the cluster with adsorption of H_2O molecule, we start with the three structures of Al_{13}^+ as stated above.

Equilibrium geometry for the configuration I of Al_{13}^+ has the skeleton of a distorted I_h geometry, and it is easy for us to specify the possible adsorption sites: top site, bridge site, and hollow site. After full optimization, the three absorptive configurations are converged to the same structure with the same energy, as shown in Fig. 4(a) (labeled as structure A), which is equivalent to configuration II of Al_{13}^+ with H_2O absorbed at the vertex atom V6. In this case, an interesting feature appears: the water molecule is preferentially absorbed on the top site, similar to water adsorption on the Al surface [24,25].

For this reason, we mainly consider top site adsorption for structure II and III. For structure II, we place the water mol-

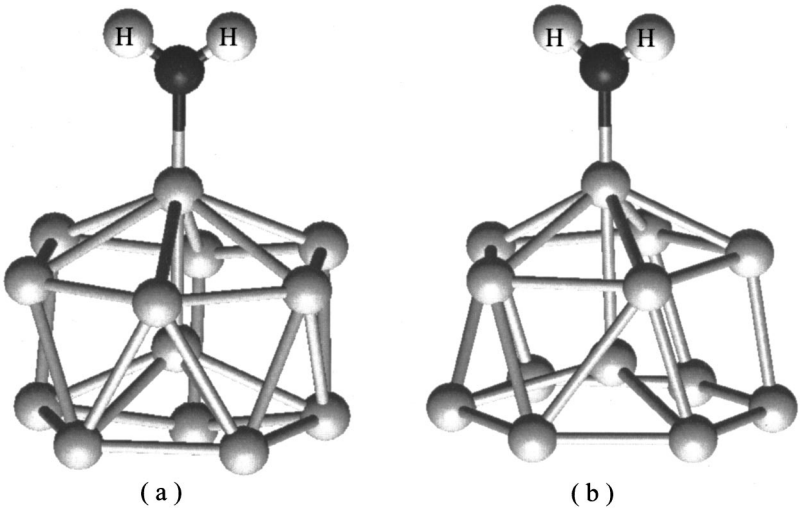

FIG. 4. Adsorption configurations of $Al_{13}^{+}H_2O$: (a) structure A, and (b) structure B.

ecule on the top site of the V6 atom as well as on the top sites of the atoms in the five-atom and six-atom rings. With full optimization, the first two converge to the structure A, while for the third one, the water molecule remains on the top site of the six-atom ring as a local minimum. The interesting point is that structure A can be obtained from several different initial configurations (top site, bridge site, and hollow site in structure I, top sites of the V6 atom and atoms in five-atom ring of structure II), which indicates clearly that the V6 atom is a preferable adsorption site for the H_2O molecule. This can be understood from the following. We know that in the case of the water molecule being on the Al surface, the main interactions involve donation of charge from H_2O to the metal [24]. Based on this, we can expect the main interactions to exist between the LUMO of Al_{13}^{+} and the lone electron pairs of H_2O, because the transferred electrons from H_2O will occupy the LUMO of Al_{13}^{+}. We found that the LUMO of Al_{13}^{+} is mainly localized on the V6 atom in structure II [as shown in Fig. 3(c)], which results in a top adsorption on V6 atom.

Similar results are also found for structure III, where the LUMO is localized on the V5 atom [see Fig. 3(d)], on to which the water molecule should be absorbed. To further examine this point, we place the water molecule on the top site of the V5 atom and the top sites of the atoms in the five-atom and the six-atom rings. We find that the first case is most stable, as shown in Fig. 4(b) (labeled as structure B). Table II lists the total binding energy, HOMO-LUMO gap, and the mean nearest-neighbor distance, as well as the adsorption energy of the water molecule, which is defined as the energy difference between the $Al_{13}^{+}H_2O$ cluster and its Al_{13}^{+} and H_2O constituents. We can see that the structure B has a larger binding energy, larger HOMO-LUMO gap, and larger adsorption energy, and, therefore, is more stable than structure A. Compared with Al_{13}^{+} cluster, the adsorption of water molecule increases the HOMO-LUMO gap to 1.634 eV, which is comparable to that of the magic C_{60} cluster. This large HOMO-LUMO gap can contribute to the stability of this cluster.

In the structure B, the distance between the V5 atom and the O atom is 1.946 Å, which is smaller than the value of 2.06 Å for H_2O bound to the Al(001) surface [24]. This occurs because the Al(001) surface has a higher coordination, and the charge density is likely to be higher; accordingly, the bond length will be elongated. In our cluster case, the H—O—H plane is tilted only 3.4° from the direction connecting the O atom and the V5 atom, which is much smaller than the corresponding values of Al(001) surface (55°) [24]. The adsorption energy is 1.772 eV, much larger than 0.53 eV for the water molecule on the Al(001) surface [24]. One of the possible reasons for this is that the Al_{13} cluster is positively charged, which creates stronger interactions with the negative lone electron pairs.

In order to check the effect of the relative orientation of H_2O molecule with the Al_{13}^{+} cluster, extensive calculations

TABLE II. Results for $Al_{13}^{+}H_2O$ cluster with structure A and B. ϵ is the total binding energy (defined respect to the isolated atoms), E_{ad} is the adsorption energy of H_2O molecule (defined as the energy difference respect to Al_{13}^{+} and H_2O), r is the average bond length between Al atoms, r(Al—O) is distance between the adsorption site and O atom, and α is the tilt angle (degrees) of H—O—H plane. The data for Al(001)-H_2O are taken from Ref. [24]. Energy is in eV and bond length is in angstroms.

Structure	ϵ	E_{ad}	HOMO-LUMO gap	r	r(Al—O)	α
Structure A	−44.6156	−1.410	1.544	2.7195	1.941	2.0
Structure B	−44.9768	−1.772	1.634	2.7064	1.946	3.4
Al(001) surface		−0.530			2.060	55

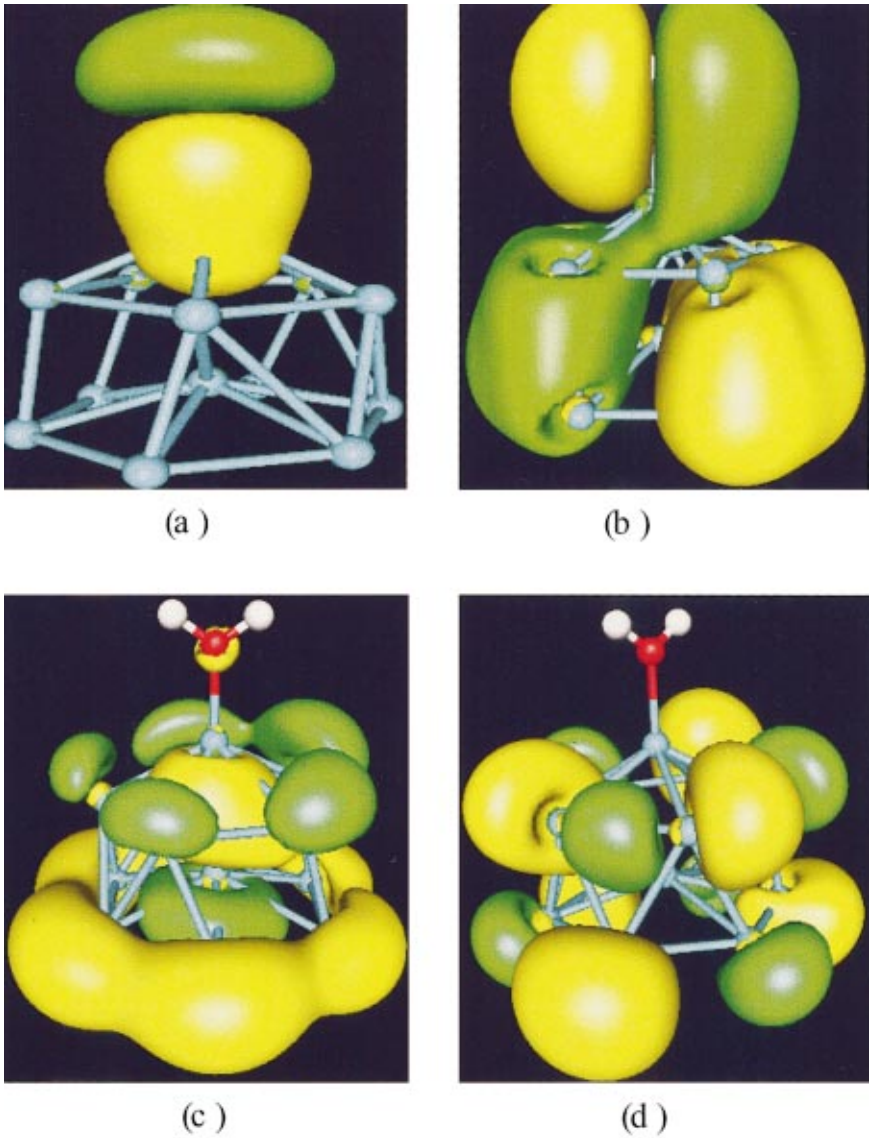

FIG. 5. (Color) (a) and (b) are the involved orbital interactions for lone pairs, and (c) and (d) for the orbitals of HOMO and LUMO in $Al_{13}^{+}H_2O$ using structure B, where the corresponding isosurface values are 0.025, 0.003, 0.02, and 0.015, respectively. Yellow is for positive, and green is for negative.

are performed in which the water molecule is tilted or rotated around the bond between the V5(6) and central Al atoms, and the structure is reoptimized. We found that the structures A and B are stable against rotation and tilting.

C. Interaction mechanism

The high stability of $Al_{13}^{+}H_2O$ cluster was tentatively explained in Ref. [7] within the jellium model. According to that interpretation, the Al_{13}^{+} cation has 38 valence electrons and hence is 2 electrons shy of the closed shell of 40. The unusually high spectroscopic intensity of $Al_{13}^{+}H_2O$ is then attributed to the formation of bond between Al_{13}^{+} and H_2O through a lone electron pair on the oxygen atom and the transfer of 2 electrons [7].

The question is how the lone electron pairs in H_2O molecule interact with Al_{13}^{+} cluster. Are the contributions from these two lone electron pairs equally important or are they biased? How many electrons are really transferred? Here we concentrate our discussions only on the most-stable structure (structure B, Fig. 4(b)). From the molecular-orbital calculations, we find that the main interactions indeed take place among the lone electron pairs in H_2O and Al_{13}^{+} cluster. The related orbitals are indicated in Figs. 5(a) and 5(b) with isosurface values of 0.025 and 0.003, respectively, which are visually quite informative. Figure 5(a) tells us that the lone electron pair with p_z character interacts mainly with the vertex V5 atom, while the lone electron pair with p_x character [the upper part of Fig. 5(b)] interacts with the main body of the Al_{13}^{+} cluster, but much more weakly than the p_z orbital. Therefore, the p_z lone electron pair dominates the interactions over the p_x, which results in two important points: (1) on top adsorption is more preferable, (2) the tilt angle of H—O—H plane is small, as we have found above. On the Al surface, the first point also holds, suggesting that the lone p_z electron pair is more important than the p_x for the interactions. However, there are more neighbors on the Al surface, and the competition between differing interactions with the two lone electron pairs produces a larger tilt angle. Mulliken population analysis indicates that there are 0.44 electrons

transferred from the H_2O molecule to the Al_{13}^+ cluster, larger than the value of 0.1 in case of Al surface [24], and different from the expectation that 2 electrons would be transferred to the Al_{13}^+ cluster [7]. Therefore, we conclude that the bonding between Al and O in the $Al_{13}^+H_2O$ cluster is covalent and not quite ionic, and the simple argument for the stability of $Al_{13}^+H_2O$ [7], which was based on jellium model, seems not to be correct. In fact, the stability for this cluster can be attributed to the large HOMO-LUMO gap and large adsorption energy. Figures 5(c) and 5(d) show the orbitals of HOMO and LUMO, which are localized mainly on Al_{13}^+.

IV. SUMMARY

In recent years, many studies have been devoted to doped Al-based magic clusters. However, $Al_{13}^+H_2O$ is the first magic Al cluster formed through molecular adsorption. In this paper, by using *ab initio* ultrasoft pseudopotential scheme complemented with molecular orbitals calculations, the structure and interaction mechanism in the magic $Al_{13}^+H_2O$ cluster are explored. The participation in the interactions of lone electron pairs results in both a large binding energy and HOMO-LUMO gap, which make this cluster very stable and magic.

ACKNOWLEDGMENT

The authors would like to express their sincere thanks to the crew of the Center for Computational Materials Science of the Institute for Materials Research, Tohoku University, for their continuous support of the HITAC S-3800/380 supercomputing facility.

[1] W. D. Knight, K. Clemenger, W. A. Heer, W. A. Saunder, M. Y. Chou, and M. L. Cohen, Phys. Rev. Lett. **52**, 2141 (1984).
[2] S. N. Khanna and P. Jena, Phys. Rev. Lett. **69**, 1664 (1992).
[3] Q. Sun, Q. Wang, J. Z. Yu, V. Kumar, and Y. Kawazoe, Phys. Rev. B **63**, 193408 (2001).
[4] B. D. Leskiw and A. W. Castleman, Jr., Chem. Phys. Lett. **316**, 31 (2000).
[5] C. Ashman, S. N. Khanna, M. R. Pederson, and J. Kortus, Phys. Rev. B **62**, 16 956 (2000).
[6] Q. Sun, Q. Wang, J. Z. Yu, V. Kumar, and Y. Kawazoe (unpublished).
[7] T. P. Lippa, S. A. Lyapustina, S. J. Xu, O. C. Thomas, and K. H. Bowen, Chem. Phys. Lett. **305**, 75 (1999).
[8] E. C. Honea, A. Ogura, C. A. Murray, K. Raghavachari, W. O. Sprenger, M. F. Jarrold, and W. L. Brown, Nature (London) **366**, 42 (1993).
[9] G. Kresse and J. Hafner, J. Phys.: Condens. Matter **6**, 8245 (1994).
[10] G. Kresse and J. Hafner, Phys. Rev. B **47**, 558 (1993); **49**, 14 251 (1994).
[11] G. Kresse and J. Furthmüller, Phys. Rev. B **55**, 11 169 (1996).
[12] N. D. Mermin, Phys. Rev. **31**, 1141 (1965).
[13] M. C. Payne, M. P. Teter, D. C. Allan, T. A. Arias, and J. D. Joannopoulos, Rev. Mod. Phys. **64**, 1045 (1992).
[14] D. M. Ceperley and B. J. Alder, Phys. Rev. Lett. **45**, 566 (1980).
[15] J. P. Perdew, in *Electronic Structure of Solids*, edited by P. Ziesche and H. Eschrig (Akademic Verlag, Berlin, 1991).
[16] M. J. Frisch, G. W. Trucks, H. B. Schlegel, G. E. Scuseria, M. A. Robb, J. R. Cheeseman, V. G. Zakrzewski, J. A. Montgomery, R. E. Stratmann, B. J. Burant, S. Dapprich, J. M. Millam, A. D. Daniels, K. N. Kudin, M. C. Strain, O. Farkas, J. Tomasi, V. Barone, M. Cossi, R. Cammi, B. Mennucci, C. Pomelli, C. Adamo, S. Clifford, J. Ciolowski, J. V. Ortiz, B. B. Stefanov, G. Liu, A. Liashenko, P. Piskorz, I. Komaromi, R. Gomperts, R. L. Martins, D. J. Fox, T. Keith, M. A. Alaham, C. Y. Peng, A. Nanayakkara, C. Gonzalez, M. Challacombe, P. M. W. Gill, B. G. Johnson, W. Chen, M. W. Wong, J. L. Andres, M. Head-Gordon, E. S. Replogle, and J. A. Pople, GAUSSIAN 98 (Gaussian, Pittsburgh, PA, 1998).
[17] C. E. Moore, *Atomic Energy Levels*, Natl. Bur. Stand. (U.S.) Circ. No. 467 (U.S. GPO, Washington, D.C., 1971), Vol. I.
[18] R. O. Jones, Phys. Rev. Lett. **67**, 224 (1991).
[19] C. A. Stearns and F. J. Kohl, High. Temp. Sci. **5**, 113 (1973).
[20] *CRC Handbook of Chemistry and Physics*, edited by D. R. Lide (CRC Press, New York, 1999), pp. 9–19, C9–23.
[21] B. K. Rao and P. Jena, J. Chem. Phys. **111**, 1890 (1999).
[22] Q. Wang, Q. Sun, M. Sakurai, J. Z. Yu, B. L. Gu, K. Sumiyama, and Y. Kawazoe, Phys. Rev. B **59**, 12 672 (1999).
[23] Q. Sun, M. Sakurai, Q. Wang, J. Z. Yu, G. H. Wang, K. Sumiyama, and Y. Kawazoe, Phys. Rev. B **62**, 8500 (2000).
[24] J. E. Müller and J. Harris, Phys. Rev. Lett. **53**, 2493 (1984).
[25] S. Q. Jin and J. D. Head, Surf. Sci. **318**, 204 (1994).